A Platform for Earthquake Risk Assessment in Iran Case Studies: Tehran Scenarios and Ahar-Varzeghan Earthquake

Babak Mansouri[1*], Amir Kiani[2], and Kambod Amini-Hosseini[3]

1. Assistant Professor and Head of Emergency Management Department, IIEES,
* Corresponding Author; email: mansouri@iiees.ac.ir
2. Ph.D. Candidate at Earthquake Risk Management Research Center, IIEES
3. Associate Professor and Director of Earthquake Risk Management Research Center, IIEES

Received: 25/01/2014
Accepted: 21/05/2014

ABSTRACT

The generation of risk maps in urban area is necessary for risk and disaster management studies and strategic planning. This research is completed in line with the tasks of the GEM-EMME (Global Earthquake Model - Earthquake Model of the Middle East) project and aims at the development of a systematic procedure in estimating the seismic risk to residential buildings and the human loss. The procedure involves four main stages. At first, the geospatial information for buildings and population are compiled and processed as to generate a country-wide geodatabase. In the next phase, ground shaking maps are produced for scenario or actual earthquakes for case studies. The third phase corresponds to the vulnerability modeling of the building stock. In the final phase, the estimate of the building damage and the associated casualty loss are calculated for two case studies. For the first case study, the residential building loss and casualty numbers are calculated for three important earthquake scenarios produced by Mosha Fault (MF), North Tehran Fault (NTF) and Rey Fault (RF) for Tehran. The current findings show that NTF can potentially account for the high number of 349428 heavily damaged or destroyed housing units and 100680 severely injured (or dead) people outnumbering MF and RF cases. For Rey fault, the estimated figures correspond to 257329 heavily damaged (or destroyed) housing units and 54468 severely injured (or dead). For the second case study, 7760 heavily damaged (or destroyed) housing units and 1045 severely injured (or dead) people are estimated for Ahar-Varzeghan earthquake (August 2012) that is in close agreement with the actual reported numbers.

Keywords:
Earthquake risk; Building inventory; Fragility curve; Vulnerability; Casualty; Risk assessment; Ahar-Varzeghan earthquake

1. Introduction

Iran is situated in highly seismic active zones and due to inadequate urban development and construction, most of the country is crucially prone to earthquake damages. In the past few decades, the country has experienced many important earthquakes comprising two major devastating events in 1990 (Rudbar-Manjil) and 2003 (Bam). For instance, the number of deaths in Rudbar-Manjil earthquake surpassed 40000 people, and more than 76% of the buildings were completely damaged in the Bam event.

Earthquake risk must be assessed in order to devise suitable mitigation strategies for both before and after disaster eras. The mitigation plan must tackle urban change and development issues (i.e. urban restructuring, reconstruction, retrofit, etc.) optimally considering actual limited resources. In that, the potential losses must also be predicted for

the benefit of post-earthquake emergency management. Earthquake losses can be assessed within regional or urban scales. Usually, for the regional scale assessment, details are traded off for the extent of the scene. For urban level analysis, the database must reflect the spatial distribution of the buildings and the population in a detailed manner. Ideally, the urban inventory must be presented and managed through well-organized geospatial databases concerning various classifications specific to the structural system, construction quality, construction age, construction materials, building height, number of floors, etc.

Successful earthquake risk and disaster management strategic planning must be backed by scientific studies and findings. During the last decade, tremendous international and national efforts were conducted in order to assess the risk and to estimate the loss for earthquake prone regions. Compiling detailed urban geospatial information has been a progressive trend for countries around the world. Systematic updating and multi-facet analysis of urban and regional data can be accomplished effectively by Geographic Information Systems. Urban risk is assessed by taking different hazard distribution maps as input and by applying suited vulnerability models to the built environment (building inventory, lifelines, industrial plant, etc.) and the population. Some risk programs are developed for academic/scientific purposes while others have been developed according to commercial or operational demands. These routines are usually adopted or can be modified for different locations around the world. Some have already a global compatibility as they incorporate world data and can support updates about desired locations. Some more advanced risk routines are spectrum-based that require detailed information about the structural seismic behavior and the ground motion. But often due to limited knowledge of the inventory and the site, macroseismic-intensity approach [1] is used. This approach relies on available empirical data derived for a specific site or inferred from similar regions where some modifications are suggested by engineering calculation or judgment.

Systematic progress of computer technology and risk algorithms has provided room for developing near-real-time loss estimation tools at local or global scales. The ShakeMap is a reference automated earthquake triggered application developed by the U.S. Geological Survey [2, 3] for rapid post-earthquake response that broadcast ground motions in near-real-time. Global Disaster Alert and Coordination System (GDACS) [4], a cooperation framework under United Nations umbrella, World Agency of Planetary Monitoring Earthquake Risk Reduction (WAPMERR) [5] and the Prompt Assessment of Global Earthquakes for Response (PAGER) [6] of USGS are examples of operating global or regional loss estimation tools. In the Euro-Mediterranean region, European agencies such as the European Mediterranean Seismological Center (EMSC) broadcast near-real-time earthquake loss estimates to emergency response institutions using some rapid loss estimation tools such as RISK-UE [1], SAFER, and LESSLOSS.

Commercial risk models with world coverage (or at least multi-country coverage) are developed by RMS, AIR, and EQECAT risk companies especially for insurance markets. EPEDAT [7] has been made for California, and alike commercial programs it offers probabilistic loss estimates as "mean loss" and "loss distribution" reporting economic loss and lifeline damage.

The Russian program EXTREMUM [8], and its alternative versions "WebLAT", and "QUAKELOSS", were made available globally to assess the consequences of strong earthquakes and devising effective response measures in an emergency. QUAKELOSS is a computer code used in estimating earthquake building damage and human losses with global coverage. This software was developed by Extreme Situations Research Center in Moscow. For this program, the world population and the built-up area databases have been compiled and stored. After taking the earthquake origin time, epicentral coordinates, the depth and the magnitude as input, the program calculates the ground shaking distribution; thereafter, building damage and casualty are estimated according to fragility curves (five vulnerability classes) and the exposure to the settlements. The loss estimation algorithm and associated functions were calibrated according to 1000 earthquakes for which losses have been reported. Therefore, the estimates are best suited for regions with frequent earthquakes.

An important widely used earthquake disaster assessment tool is the HAZUS [9] methodology developed by Federal Emergency Management

Agency (FEMA). HAZUS-MH (NIBS and FEMA 2003) is a multi-hazard methodology that contains models for estimating pre-event potential losses or physical, economic, and social impacts from earthquakes, floods, and hurricanes using Geographic Information Systems (GIS) technology. The Australian EQRM, the Norwegian SELENA, and the Turkish HAZTURK are all based on the HAZUS methodology but tailored specifically for those countries. For example, SELENA (Seismic Loss Estimation using a logic tree Approach) is developed at NORSAR through support from the International Centre for Geohazards, Norway. The software is a Matlab™ [10] based computer tool, structured according to HAZUS methodology for computing damage scenarios. The ground motion and fragility curves are adjusted primarily for Norway conditions but can be modified by the user as needed.

MAEViz [11] is a platform for seismic risk assessment developed in the Mid-America Earthquake (MAE) Center research in the United States. This is an open-source and extensible software platform that integrates latest research findings, updated accurate data, and novel methodologies for risk computation.

SERGISAI (SEismic Risk evaluation through integrated use of Geographical Information Systems and Artificial Intelligence techniques) is a computer code for seismic risk assessment funded by the European Commission [12]. One important goal of this project is to improve the communication between the scientific community and the public administrations and decision makers. End users can perform risk assessment at local, sub-regional and regional geographical scales. Risk is expressed in terms of expected damage relative to hazard and vulnerability. Both the probabilistic and the deterministic approaches were implemented for the hazard computation.

SIGE-ESPAS is a near-real-time loss estimation software developed by the Italian Civil Protection for emergency planning. The vulnerability model is derived from damage surveys of about 50,000 buildings in destructive Italian earthquakes. The loss model is intensity-based and according to empirical fragility curves derived by Sabetta et al. [13]. Losses are expressed in terms of the number of damaged dwellings, direct monetary losses, and casualty.

ESCENARIS is developed by the Geologic Institute of Catalonia in Spain and has been used for Catalonia emergency plan [14], a rapid response system [15], and SES 2002 software [16] for the Spanish Civil Protection.

TEDES (Tehran Earthquake Damage Estimation System) is a near-real-time monitoring system launched by the municipality of Tehran to augment its disaster management effectiveness through different consequence-based exercises or actual monitoring of real events. The system is capable of integrating different networks of seismographs or producing simulated ground shaking for different scenarios. The system incorporates updatable geospatial urban inventory in addition to vulnerability functions tailored for Tehran.

ELER (Earthquake Loss Estimation Routine) [17] was developed under the Network of Research Infrastructures for European Seismology-NERIES. This is a multi-level routine primarily intended for post-earthquake rapid loss estimation, but equally feasible for scenario-based loss assessments. Level 0 is similar to PAGER system of USGS and uses regionally adjusted intensity-casualty or magnitude-casualty correlations. Level 1 takes as input regional building inventory databases for reporting building damage and casualties. Level 2 analysis can be performed according to Capacity Spectrum Method, Modified Acceleration-Displacement Response Spectrum Method, Reduction Factor Method and Coefficient Method similar to HAZUS and SELENA for concluding building damage and consequential human casualties (ELER© v3.0, 2010).

GEM (Global Earthquake Model) [18] consists of different regional earthquake models covering the globe. For the Middle East region, EMME (Earthquake Model of Middle East) is coordinated by Kandilli Observatory and Earthquake Research Institute of Turkey (KOERI) [19] with the participation of institutions from International Institute of Earthquake Engineering and Seismology (IIEES) of Iran, NED University of Pakistan, Jordan University of Science and Technology of Jordan, American University of Beirut of Lebanon, Cyprus University of Technology of Cyprus, Ivane Javakhishvili Tbilisi State University of Georgia, National Academy of Sciences of Armenia, and National Academy of Sciences of Azerbaijan. This project consists mainly of Seismic Hazard and Risk work packages. According to the risk assessment module (WP4 - Work Package 4) [1], the development of a systematic pro-

cedure is sought for estimating the seismic risk to residential buildings and the human loss tailored for the country. In this investigation and in line with WP4, a country-wide risk assessment methodology is devised considering the availability, coverage and the quality of spatial data for Iran. In general, lifeline systems are regarded as main components for integrated seismic risk assessment; however, the platform is tailored and operated for estimating loss to residential buildings and casualty at this time. Nevertheless, it should be mentioned that the risk assessment platform has the capability of assessing damage to pipelines according to PGV distribution together with pipeline database (with ductility properties such as brittle-ductile table). But, due to the lack of data and complexity of procedure, other lifeline components have not been modeled yet.

Exposure modeling for both residential buildings and population is performed by joining national (but very coarse) databases with statistical measures and dasymetric models such as Landscan [20]. This created a unique geospatial database for the entire country with uniform resolution without limitation for future adjustment and refining. The evaluation of the risk is provided according to the nature and the contents of the data sets. The database for the exposure database is refined as to represent the effective taxonomy. This categorization implies not only the nominal structural types but also reflects the quality and the age of the construction. New sets of vulnerability curves are derived and presented according to EMS-98 scales that can be compared with such functions for other parts of the world. These functions are described by Beta distribution as complemented by other distribution function or empirical results. Moreover, such country-wide implemented platform is unique as it is created for the first time for the country, provided unmatched feasibility in computing risk or damage according to different possible scenarios.

As case studies, risk assessment results for Tehran concerning important earthquake scenarios and loss estimation of the 2012 Varzeghan earthquake are reported in this paper. Briefly, this requires the development of ground motion maps, building inventory databases and vulnerability functions to be used in an earthquake loss estimation routine such as ELER. In the following sections, the methodology for developing the "Elements at Risk" databases and the procedure for deriving the vulnerability functions are described. Then, the "Implementation and Results" section provides our findings regarding the vulnerability parameters and curves designated for Iran. The last part discusses the application and the results for the case studies.

Nevertheless, it should be pointed out that the nature of seismic risk assessment reflects degrees of aleatory and epistemic uncertainties. For example, input events, occupancy pattern, material strength and behavior during shaking exhibit randomness. On the other hand, lack of knowledge in understanding properly and precisely all mechanisms involved in a destructive event such as earthquake as well as any imperfection in modeling the integrated risk causes inaccuracy. Some levels of uncertainty can be associated by each risk component as: 1) in hazard calculation - earthquake magnitude, fault geometry, fault mechanism, depth, site effects, attenuation relationship…, 2) for elements at risk databases development - lack of or misregistered geospatial data, errors in statistics, data model and data distribution errors, and 3) for vulnerability and human loss computation - capacity curves, demand curves, lack of empirical data and developing data models (although empirical results are uncertain as well).

2. Methodology

Ground motion maps refer to the distribution of ground motion parameters (PGA, PGV...) or seismic intensities. The estimation of ground shaking is carried out according to the fault parameters, recent NGA (Next Generation Attenuation) relations and GMPEs (Ground Motion Prediction Equations), and site effect. This topic is elaborated in the case study section for it refers specifically to the scenario earthquakes of interest.

In compiling the exposure data, residential building inventory and demographic geodatabases were completed for the country. For this purpose, a complete set of census data and associated spatial information were analyzed. Moreover, the database was conditioned according to a global population distribution standard (LandScan, ORNL) that represents the finest residential resolution as uniform grids.

Due to the limited knowledge regarding the inventory and the site effects, macroseismic intensity approach is used in this investigation. This approach

relies on available empirical data derived for a specific site or inferred from similar regions where some modifications are suggested by engineering calculation or judgment. Nevertheless, in some instances, the spectrum-based fragility curves are used as a base for calibration.

2.1. Exposure - Elements at risk

The database development is dependent on the type and the quality of the available data. For Iran, only a few cities have compiled parcel records with acceptable geometric and attribute details. Nonetheless, these data sets are not accessible yet. National population statistics records are updating based on the decennial census program. Although the data is collected using questionnaires on a door-to-door basis, the results are presented and disseminated as aggregates of geographic units. These geographic units are usually census tracts or city blocks. Apparently, there is an essential need in distributing the population according to much finer resolutions. For mapping the population density relative to residential land-use, the dasymetric mapping technique can be utilized where a coarse spatial data is disaggregated to finer spatial units that exhibit relative homogeneity. This process involves the use of suitable ancillary data sets.

The latest census data is published for 2006. "Population" and "Building" (housing units) data sets are summarized within provinces, metropolitan areas, urban and rural settings. The data is gathered by questioning individual households. The other source of information is derived from the PARS digital database package where some useful census data were overlaid on geographic or administrative boundaries using GIS compatible shape files. The whole spatial data sets are georeferenced and controlled for possible flaws. The initial statistics is presented as points within rather large geographic extents; therefore, additional spatial data was essential to distribute the aggregated data within adequate spatial grids. For this purpose, LandScan (2008)TM data was utilized which represent initially the ambient population (average of 24 hours) within grids of 0.5 arcmin or 0.0083^{o} for Iran. LandScan is a global population distribution standard that uses a combination of GIS and remote sensing data and techniques where mid-resolution (30 meters) and very high resolution VHR (1 meter) imageries and image processing algorithms are utilized to detect surficial features.

Four types of general building taxonomy represent the structural typology effectively. It is noticed that the census data reflects the building typology for each housing unit and not for individual buildings. The four major building categories are adobe, masonry, reinforced concrete and steel. Three construction time intervals namely "before 1976", "1976-1996", and "1996-2006" reflect different levels of earthquake resistant design (ERD) or construction quality as "Low Code", "Moderate Code" and "High Code". Table (1) summarizes the building taxonomy for Iran.

The development of residential building stocks and the population databases has been already reported [21] where the country geodatabase is provided according to ~1 km and ~5 km grids.

2.2. Vulnerability Modeling

The procedure includes the derivation of vulnerability curves for some most common structural types. Empirical fragility curves are generally preferred for regions that have experienced devastating earthquakes in the past. However, because such data is not available for Tehran, some analytical results are proposed. These curves are compared

Table 1. Comparison of Damage States/Grades in ATC-13, HAZUS and EMS-98.

ATC-13			HAZUS		EMS-98		
Damage State	**Damage Factor Range (%)**	**Central Damage Factor (%)**	**Damage State**	**Central Damage Factor (%)**	**Damage Grade**	**Damage Factor Range (%)**	**Central Damage Factor (%)**
Slight	0-1	0.5	Slight	2	D1: Slight	0-1	0.5
Light	1-10	5					
Moderate	10-30	20	Moderate	10	D2: Moderate	1-20	10
Heavy	30-60	45	Extensive	~ 50	D3: Substantial to Heavy	20-60	40
Major	60-100	80	Complete	100	D4: Very Heavy	60-100	80
Destroyed	100	100			D5: Destruction	100	100

and adjusted with the empirical data from the devastating Manjil, Iran Earthquake of 1990 [22] and with the vulnerability results for the concrete buildings destroyed in Kocaeli, Turkey earthquake of 1999 [23]. A set of vulnerability or fragility curves are presented for the existing building typologies. These functions are derived using the EMS-98 [24] procedure but with some modifications according to empirical or analytical results or expert judgment.

A reference empirical damage function for Iran is based on the results of the devastating Manjil-Rudbar earthquake in Iran that occurred in June 1990 [22]. In the above-mentioned reference, the iso-damage zoning map for buildings was compiled in conjunction with the study of a number of ground motion records. The related building pool was a mix of three categories: a) steel and concrete frames (10.4 %), b) semi-engineered, also categorized as masonry or wood (83.1%), and c) non-engineered as adobe (6.5%). This reference empirical damage ratio curve represents heavily damaged or collapsed buildings for a given peak ground acceleration and has been used in this research for tuning some analytically derived vulnerability curves.

Structural fragility curves were developed according to the mechanical method (capacity-demand spectrum method) considering building taxonomy and site conditions for Tehran [25]. The capacity curve is a simplistic representation for the dynamic behavior of the entire structure by considering a SDOF system. The capacity curves are determined by two sets of points, the yield and the ultimate capacity points, where the first indicate the limit for linear response and the second is related to the nonlinear part of the capacity curve. The seismic demand spectrum was derived according to FEMA NEHRP-97 procedure were the spectral acceleration was calculated for 0.3 s and 1.0 s periods (Sa@0.3s, Sa@1.0s) for different zones within the study area. Utilizing the selected GMPEs (described in the previous section), three different spectral acceleration maps were created and the average values of the spectral accelerations were calculated for each earthquake scenario.

As a requirement for the GEM-EMME project, intensity-based vulnerability curves were also developed in this research. The process for developing such curves usually requires detailed empirical damage data that is generally missing for Iran earthquakes. However, the intensity-based curve parameters are derived by comparing the results of the mechanical modeling and some available damage curves.

2.3. Fragility Curve Derivation - Mechanical Modeling (Spectrum-Based)

In order to generate the fragility curves by the spectrum-based mechanical modeling, the capacity and the demand curves are interacted together till the equilibrium is reached between the dissipated hysteretic energy of the structure and the demand curve considering effective damping [26]. The equilibrium points (median spectral acceleration $\bar{S}_{a,ds}(g)$) are considered as the median spectral displacement, $\bar{S}_{d,ds}(in)$, in the ADRS (acceleration displacement response spectra) coordinate system. These values are computed for different building typologies and consequently, the lognormal fragility curves are obtained for four damage states namely, Slight, Moderate, Extensive and Complete using a standard deviation of 64% according to expert judgment. The probability of being in or exceeding a specified damage state is modeled as a cumulative lognormal distribution as bellow:

$$P\langle ds|S_d\rangle = \Phi\left(\frac{1}{\beta_{ds}}\ln\left(\frac{S_d}{\bar{S}_{d,ds}}\right)\right) \quad (1)$$

$\bar{S}_{d,ds}$: median value of spectral displacement at threshold of damage state *ds*,

β_{ds}: standard deviation of natural logarithm of spectral displacement of damage state, *ds*,

Φ: standard normal cumulative distribution function.

2.4. Fragility Curve Derivation - EMS-98 Method (Intensity-Base)

This is a semi-empirical method where the mean damage of a specific building type is determined by the vulnerability and quality indices and the earthquake intensity. Using these parameters and considering the Beta distribution function, damage probability matrices and fragility curves are derived. The following three steps are involved in producing the fragility curves according to EMS-98 methodology (RISK-UE 2003):

- **Step1:** Estimation of the total vulnerability index where total vulnerability index is defined as:

$$\overline{V}_I = V_I^* + \Delta V_m + \Delta V_R \quad (2)$$

V_I^* : suggested values by EMS-98 for the European structural types

ΔV_m : modification factor

ΔV_R : regional adjustment factor

- Step 2: Estimation of the mean damage grade:

$$\mu_D = 2.5\left[1+\tanh\left(\frac{I+6.25\overline{V}_I-13.1}{Q}\right)\right] \quad (3)$$

I: intensity in EMS-98 scale

Q: quality index

- Step 3: Estimation of the damage distribution (damage probability matrix and fragility curves):

$$PDF: p_\beta(x) = \frac{\Gamma(r)}{\Gamma(r)\Gamma(t-r)}\frac{(x-a)^{r-1}(b-x)^{t-r-1}}{(b-a)^{t-1}} \quad a \le x < b \quad (4)$$

$$CDF: P_\beta(x) = \int_a^x p_\beta(\alpha)\, d(\alpha) \quad (5)$$

where: $a=0; b=6; t=8; r = (0.007\mu_D^3 - 0.052\mu_D^2 + 0.2875\mu_D)$

PDF: Probabillity Density Function;

CDF: Cumulative Density Function

3. Implementation and Results

3.1. Fragility Curves - Spectrum-Based Parameters

Interacting the capacity and the demand curves, the equilibrium points (median spectral acceleration ($\overline{S}_{a,ds}$ (g)) are considered as the median spectral displacement ($\overline{S}_{a,ds}$ (in)) in the ADRS (acceleration displacement response spectra) coordinate system. These values are computed for different building typologies and consequently, the lognormal fragility curves are obtained for four damage states namely, Slight, Moderate, Extensive and Complete, Table (2). For example, Figures (1) and (2) depict the "Complete" damage state fragility curves for low-rise and mid-rise buildings for some selected masonry

Table 2. Median Spectral Displacement and Median Spectral Acceleration for selected building Types.

Building Type	Median Spectral Displacement (in) Median Spectral Acceleration (g)	Probability of Damage			
		Slight	Moderate	Extensive	Complete
S1	$\overline{S}_{d,ds}(in)$	2.16	4.02	9.63	25.21
	$\overline{S}_{d,ds}(g)$	0.15	0.25	0.48	0.96
S2	$\overline{S}_{d,ds}(in)$	1.08	2.16	5.40	12.60
	$\overline{S}_{d,ds}(g)$	0.10	0.18	0.32	0.52
S3	$\overline{S}_{d,ds}(in)$	0.86	1.75	4.32	10.08
	$\overline{S}_{d,ds}(g)$	0.08	0.16	0.26	0.42
C1	$\overline{S}_{d,ds}(in)$	1.50	2.80	8.00	21.00
	$\overline{S}_{d,ds}(g)$	0.15	0.27	0.58	1.12
C2	$\overline{S}_{d,ds}(in)$	0.90	1.80	4.50	10.50
	$\overline{S}_{d,ds}(g)$	0.09	0.13	0.19	0.26
C3	$\overline{S}_{d,ds}(in)$	0.72	1.44	3.60	8.40
	$\overline{S}_{d,ds}(g)$	0.07	0.10	0.16	0.21
M1	$\overline{S}_{d,ds}(in)$	0.48	1.26	3.15	7.35
	$\overline{S}_{d,ds}(g)$	0.09	0.14	0.19	0.27
M2 & M3	$\overline{S}_{d,ds}(in)$	0.50	1.01	2.52	5.88
	$\overline{S}_{d,ds}(g)$	0.09	0.12	0.16	0.22
Ad	$\overline{S}_{d,ds}(in)$	0.32	0.65	1.62	3.78
	$\overline{S}_{d,ds}(g)$	0.12	0.19	0.25	0.28

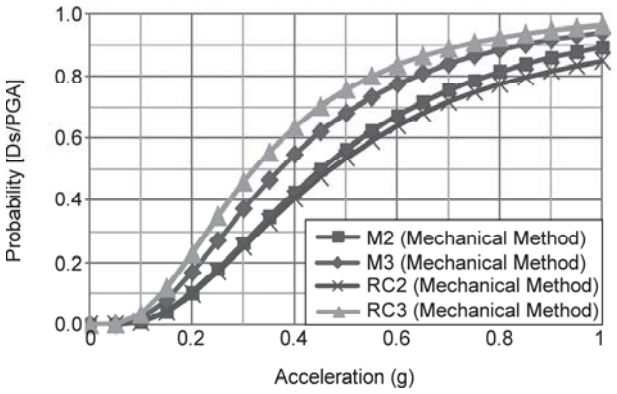

Figure 1. "Complete" damage state fragility curves for selected low-rise buildings [27].

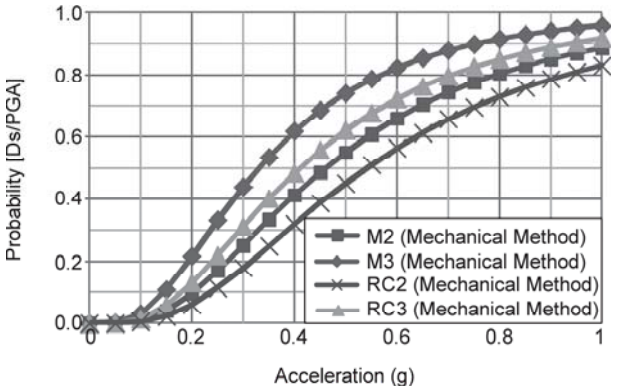

Figure 2. "Complete" damage state fragility curves for selected mid-rise buildings [27].

and concrete structures. In there, the capacity curves were constructed according to the parameters suggested by the HAZUS-MH procedure as confirmed by expert opinion for the target taxonomy [27]. The demand curves were constructed based on the FEMA NEHRP-97 methodology considering the site condition [27].

3.2. Fragility Curves - Macroseismic-Intensity Parameters

The overall damage distribution can be described by a single parameter called the mean damage ratio (MDR). This is the weighted average of the central damage factors or central damage ratios (CDR) for all Damage States (DS) at each intensity level (I).

In this research, all comparisons and calibrations are performed using the MDR curves. Considering different levels of damage (or damage grades), the mean damage ratios, and conversion between MDR values with damage state fragility curve values, Table (1) is used.

The intensity levels in MMI and EMS-98 scales are taken almost identical. Table (1) compares damage states, damage grades, damage factor ranges and their related central damage factors in ATC-13 [28], HAZUS and EMS-98 methodologies. This table is used to select and compute the combination of different damage grades when calibrating the results with a reference function is in mind. For example, given that the reference curve describes the combined damages for "extensive to complete" (HAZUS terminology), the combined Mean Damage Ratio pronouncing D3 to D5 damage grades must be sought in order to derive the fragility curves in EMS-98 system.

The "Behavior Modifier" ΔV_m was selected for three levels of ERD quality. ΔV_R or the "Regional Modifier" was introduced to modify the vulnerability index according to expert judgment or observed vulnerability results specific to the region of interest. For calibrating the preliminary EMS parameters (V_I^* and Q) with respect to each designated damage curve, ΔV_R values are incrementally varied and the above three steps were involved until the modified EMS-98 curves matched with the target curves. This is by setting a threshold value for error calculation between the curves. Table (3) lists the vulnerability indices for the designated building stock.

As they are practically compatible, intensity levels in MMI and EMS-98 scales are taken identical. The Turkey URM (Unreinforced Masonry) collapse probability curve (Figure (3)), and M2 and M3 curves derived from mechanical modeling (Figure (1)) were compared together after converting PGA and MMI units using Trifunac and Brady [29] data model. The comparison showed a close match between these curves.

In many cases, the method specific (i.e. HAZUS versus EMS-98) comparison between fragility curves must be performed in order to complete the fragility catalogue for the entire building stock. Also in many cases, damage ratio curves must be compared with fragility curves and this imposes a conversion process. The mean damage ratio curve can be derived by the summation of the probability of each damage state weighted by the corresponding central damage ratio. As an example, Figure (4) shows the fragility curve for four levels of physical damages according to HAZUS terminology for M3 (unreinforced masonry). The weighted combination of Extensive and Complete damages in HAZUS can

Table 3. Calibrated vulnerability indices according to EMS-98 with regional modification.

Typology	Description	Earthquake Resistant Design Level	Building Height	Quality Index (Q)	Vulnerability Index (V)			
					Vuln. Index (VI*)	Behavior Modifier (? Vm)	Regional Modifier (? VR)	Total Vulnerability Index (V)
Ad	Adobe	-	Low	1.80	0.84	0	0.160	1.00
M1	Reinforced Masonry Walls	(High Code)	Low	2.3	0.451	0	0.179	0.63
M2 & M3	Unreinforced Masonry	(Pre or Low Code)	Low	2.00	0.776	0	0.114	0.89
RC1	RC Frame + Infill Walls	(High Code)	Medium	2.3	0.442	- 0.16	0.338	0.62
RC2	RC Frame + Infill Walls	(Medium Code)	Medium	2.0	0.442	0	0.248	0.69
RC3	RC Frame + Infill Walls	(Pre or Low Code)	Medium	2.0	0.442	+ 0.16	0.218	0.82
S1	Steel Frame Braced Steel Frame + Infill Walls	(High Code)	Medium	2.3	0.484	0	0.106	0.59
S2	Steel Frame + Infill Walls	(Medium Code)	Medium	2.1	0.484	0	0.266	0.75
S3	Steel Frame + Infill Walls	(Pre or Low Code)	Medium	2.0	0.484	0	0.336	0.82

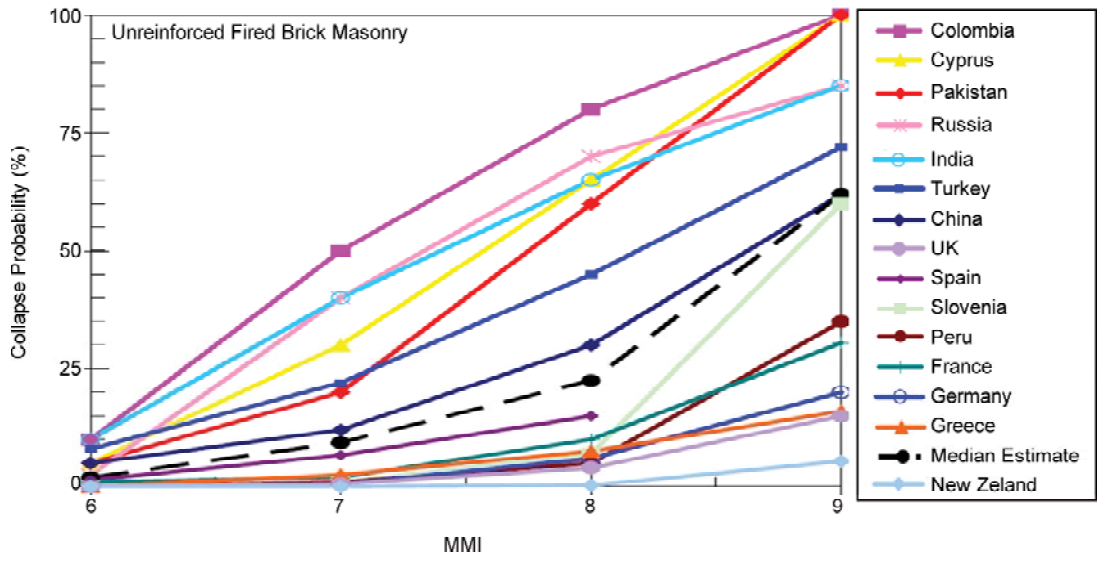

Figure 3. Collapse fragility of unreinforced fired brick masonry construction, estimated by 16 WHE (World Housing Encyclopedia) experts [30].

be taken equivalent as the weighted combination of D3 to D5 fragility curves in EMS-98 method. As a result, the damage curves for M2 and M3 (mechanical method) structures are derived as shown, Figure (5). An empirical curve obtained from the Rudbar-Manjil earthquake [22] is compared with four analytically derived curves and shows close match with M2 and M3 cases.

To justify the values for the parameters listed in Table (1), the following description is presented. For Adobe structures, ΔV_R and Q are selected as 0.16 and 1.8 respectively. For M2 and M3, is calculated as 0.114 that shows a shift of the initial EMS curve to the left ΔV_R and Q of 2.00 to be adjusted for the slope. Because of the lack of data, the calibrated M1 building (high quality Masonry) curve is constructed from EMS-98 curve (Table (1)) but with a shift of two units to the left according to the ATC-13 suggestion (considering low quality of regional materials or construction methods). This shift is equivalent to a ΔV_R of 0.179.

Figure (6) shows sets of vulnerability curves for

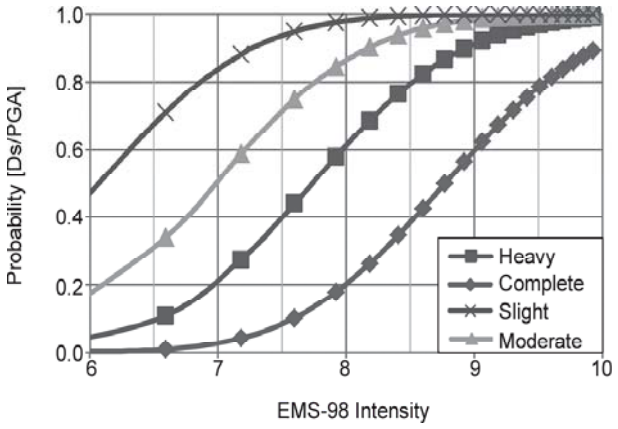

Figure 4. Fragility curve for M3 (Mechanical Method) building type derived by mechanical modeling.

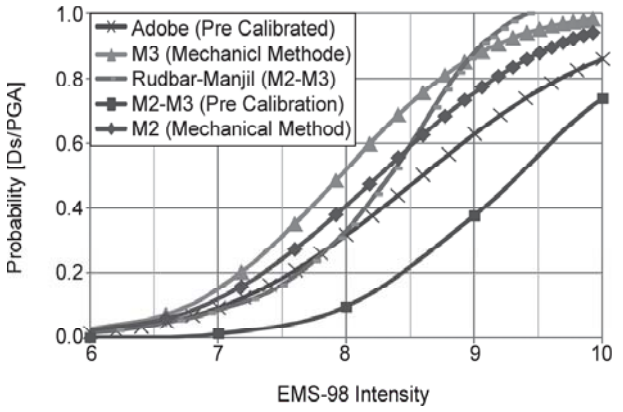

Figure 5. Damage curves for M2 and M3 (mechanical method), empirical (Rudbar-Manjil curve), M2 and M3 (EMS-98 method) and Adobe (EMS-98).

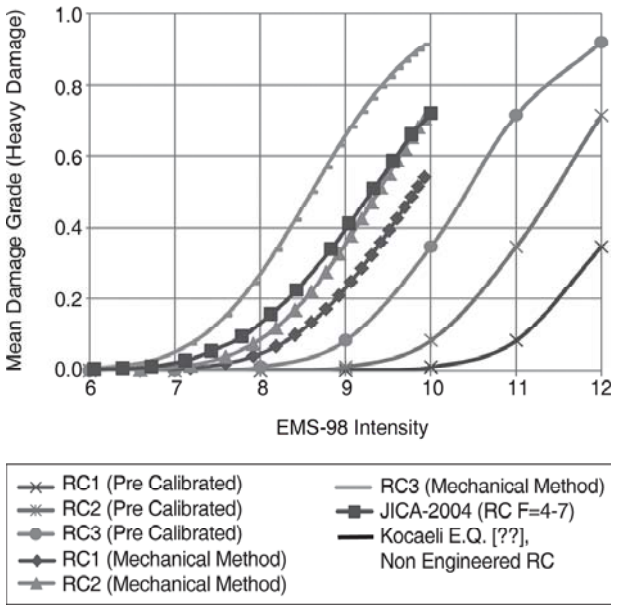

Figure 6. Vulnerability curves for R/C buildings according to mechanical modeling, preliminary EMS-98 parameters, JICA-2004 and empirical data of Kocaeli 1999 earthquake.

R/C buildings derived from mechanical modeling, preliminary EMS-98 parameters, JICA-2004 [31] study and empirical data of Kocaeli earthquake 1999 [23]. For RC1 typology, the EMS parameters are adjusted according to the mechanical model using of 0.338. For RC2 curve, the Kocaeli earthquake data and the result of JICA-2004 study match closely with the mechanical modeling, thence the EMS parameters are adjusted according to of 0.248 ΔV_R and Q value of 2.0. However, for RC3, to take into account for shift and slope of the curves, both the vulnerability and quality indices are adjusted considering 0.218 and 2 values for ΔV_R and Q respectively.

For S1 buildings, S2M-High-Code (Mechanical Method) is used with ΔV_R of 0.106. For S2 buildings, S1M-Mod-Code (Mechanical Method) is used, and ΔV_R is equivalent to 0.266, and also the "Q" value has been changed to 2.1 to be adjusted for the slope of the curve. And for S3 buildings, S5M-Low-Code (Mechanical Method) is used with ΔV_R equivalent to 0.336 and the "Q" value has been changed to 2 to be adjusted for the slope of the curve. Figure (7) shows the EMS compatible vulnerability functions according to the vulnerability parameters adjusted for Iran. These curves were derived for the entire building taxonomy.

4. Case Study 1 - Tehran

4.1. Seismogenic Sources and Hazards

Faults- Important active faults are studied in the vicinity of Tehran. Based on some previous studies

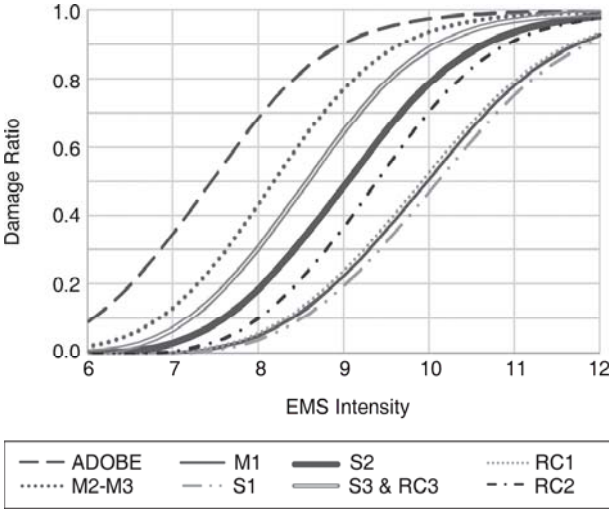

Figure 7. Calibrated vulnerability curves according to EMS-98.

by JICA-2000 [23], the most probable hazardous faults are known as Mosha (MF), North Tehran (NTF) and Rey (RF) faults. These faults are graphically shown in Figure (8). The faults' lengths, origins and azimuths were determined from surface fault traces. The faults' widths and earthquake moment magnitudes were determined by faults' lengths using empirical relationships according to Wells and Coppersmith [32].

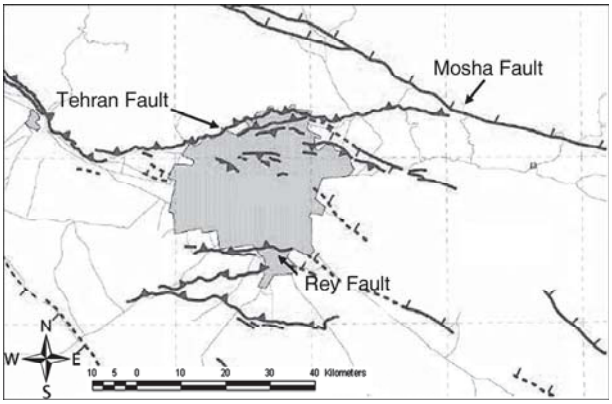

Figure 8. Tehran and corresponding known active faults (courtesy of IIEES).

More recently, Gholipour et al. [33] have reported these faults' parameters as shown in Table (4). Noting that MF and NTF have higher lengths and annual slip rates, these can be considered as more seismically active than RF.

In another study, a network of 54 survey GPS sites were implemented in addition to 28 continuous GPS receivers and three absolute gravity observation to reveal the kinematics in the Alborz mountain range [34]. The sensors were installed within 10km distance apart near Tehran and sparser elsewhere. The measurements were made between 2000 and 2008. The observed slip rates are in agreement with the study reported by Gholipour et al. [33].

4.2. Site Effect

The assessment of seismic site conditions is valuable in obtaining realistic ground-motion maps. For a specific area of interest, conventionally, large amount of data sets (i.e. borehole data) and sophisticated computations are required for calculating the seismic site effects. For the cases where there is no such detailed information available, or in an attempt to simplify the site effect modeling, Wald and Allen [2] describe a methodology based on topographic slope information. The average shear wave velocity down to 30 m (Vs30) is correlated with topographic slope. In that, two sets of parameters were derived for active tectonic and for stable continental regions. In this research, the Vs30 map of Iran is provided by the USGS according to above mentioned method. The Vs30 map of Iran and Tehran are provided by the USGS source as depicted in Figure (9).

Some Vs30 zonation studies are completed for Tehran by different researchers. As a highlight, Shafiee and Azadi [35] estimated the Vs30 for Tehran according to the NEHRP method using 169 seismic refraction tests and 19 downhole tests performed during 1995 till 2004. Ghayamghamian et al. [36] completed a study in determining the soil amplification factor for Tehran. In that the result of 208 seismic profiles was obtained from 137 seismic refraction tests and 71 downhole measurements distributed within Tehran. The soil classification was according to the NEHRP and the 2800 Standard methodologies as such the shear wave velocity was estimated for six geological units. As a result, the shear wave velocity down the first 30 meters of subsoil was mapped for the extent of Tehran by interpolation.

Although there may be some more reliable results obtained for Tehran or other parts of Iran, but due to some experienced limitations, the topo-

Table 4. Seismic parameters for three major faults in greater Tehran region (courtesy of Gholipour et al. [33]).

Fault Name (Abbreviation)	Fault Length (km)	Moment Magnitude Mmax (Mw)	Mechanism	Elastic Thickness (km)	Horizontal Slip Rate (mm/y)	Slip on Fault (mm/y)
Mosha (MF)	79	7	S	15	-	1.00-2.30
N. Tehran (NTF)	59	7.1	T/S	15	0.70-1.00	1.55
N. Rey (RF)	25	6.7	T	15	0.30	0.35

S: Strike-slip mechanism T: Thrust mechanism

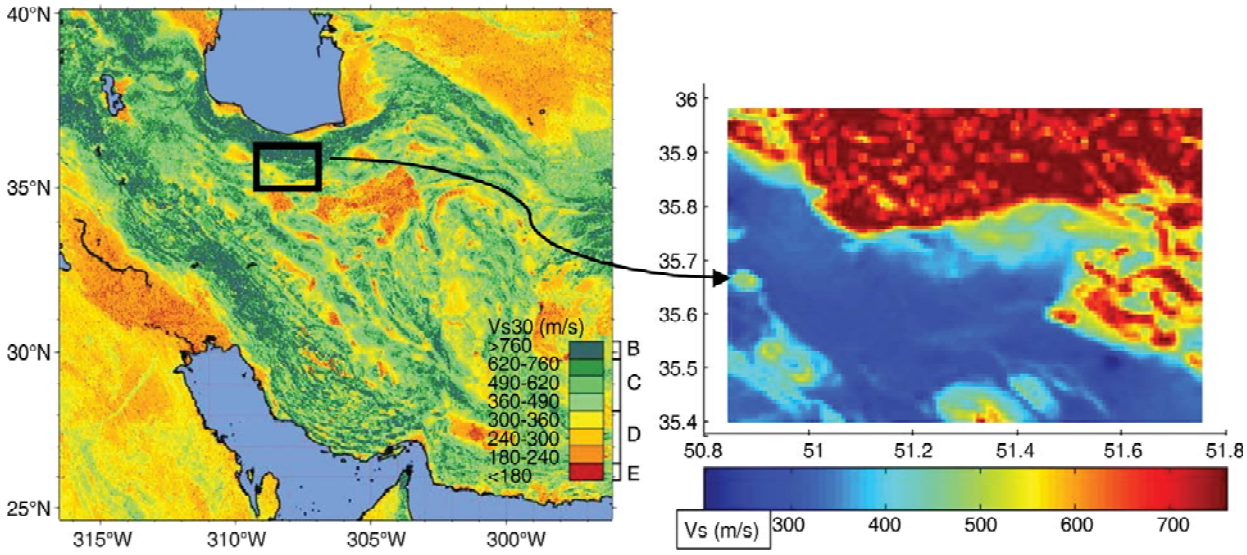

Figure 9. Upper 30-m average shear wave-velocity (Vs30) for Iran & Tehran (USGS data).

graphic-based Vs30 of USGS was utilized in this study. The USGS map has a country-wide coverage with the option of adjusting and correcting for specific part as needed. The preliminary purpose of this study was to make operational a country-wide comprehensive model with the cost of losing some precision. Nevertheless, for future development and upon access to more reliable input data, the database can be improved as needed.

The Next Generation Attenuation (NGA) relations and GMPEs provide means for computing the ground motion parameters at the ground surface by taking into account the local site effects (i.e. Vs30 parameter) as feasible and implemented in this platform. In this research and for the studied cases, Boore et al. [37] relation is selected for predicting the ground motion and Wald et al. [38] equation is used for producing the instrumental intensity at the ground surface. A major benefit in using such a methodology is the speed and the ease of implementation. Figures (10) and (11) show the PGA maps for NTF and RF scenarios.

5. Distribution of Building Damage and Casualty for Tehran

In the previous sections, the procedure for

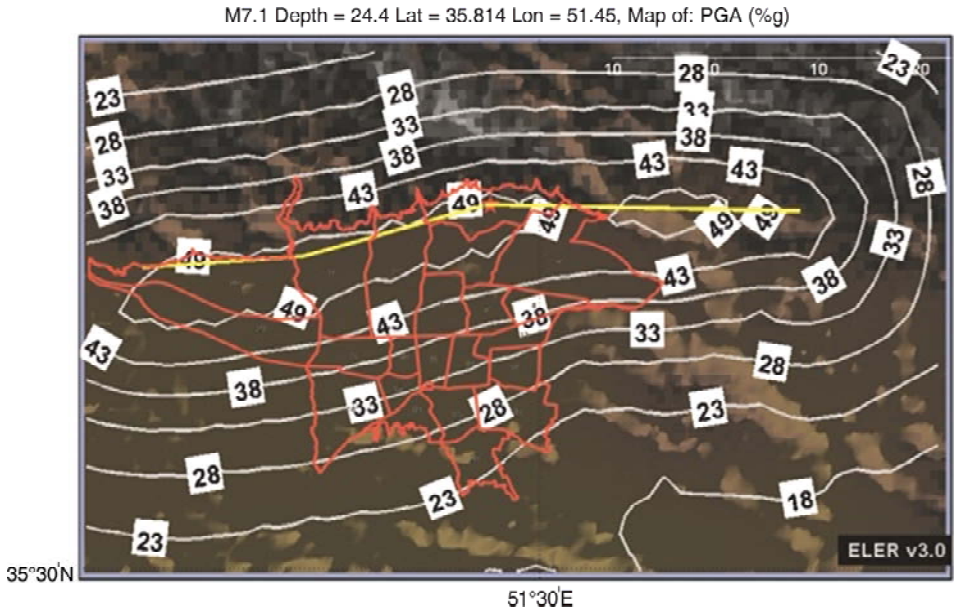

Figure 10. PGA contour map for NTF scenario.

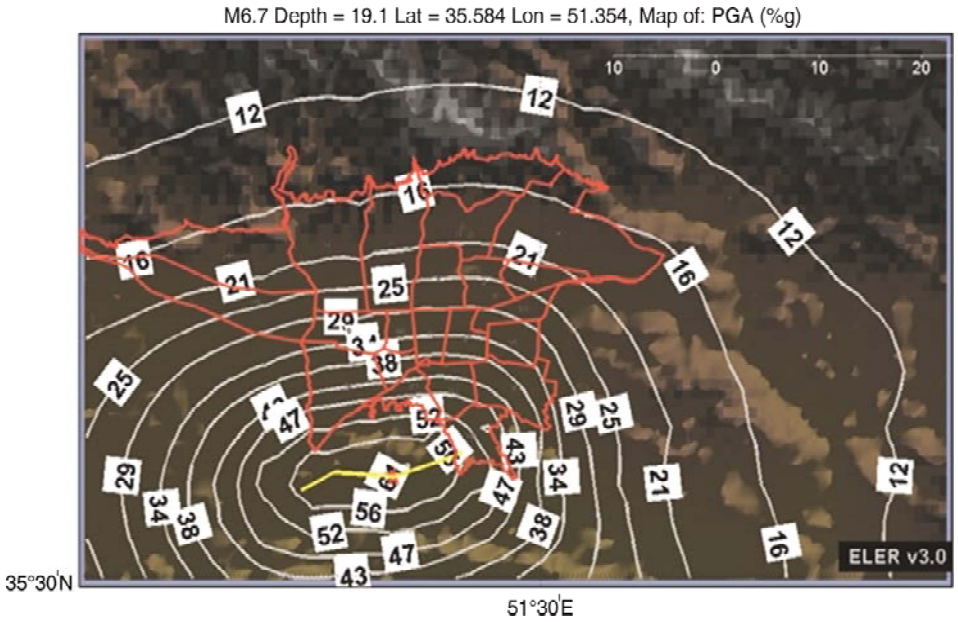

Figure 11. PGA contour map for RF scenario.

estimating the ground motion at the surface, the development of the country-wide exposure databases for residential housing units and the population as well as the derivation of the structural vulnerability curves were explained. The outcome of the scenario earthquakes can be calculated by combining the above information in an integrated system such as a GIS. In this research, the Earthquake Loss Estimation Routine (ELER© v3.0, 2010) has been used. The shake mapping methodology in this software is similar to the USGS Shake Map. For its importance, Tehran has been selected as the study area where the impacts of three major known faults were studied. The study reflects the housing damage distribution according to damage grades "D4" and "D5" described as "very heavy damage" and "destruction" respectively. Additionally, the human loss is computed based on the building damage using Coburn and Spence [39] method. The distribution of housing unit damages (damage grades of D4+D5) is shown for RF, TF and MF scenarios in Figure (12) through Figure (14). The results for damages to residential housing units and human casualties are compared in more details in Table (5).

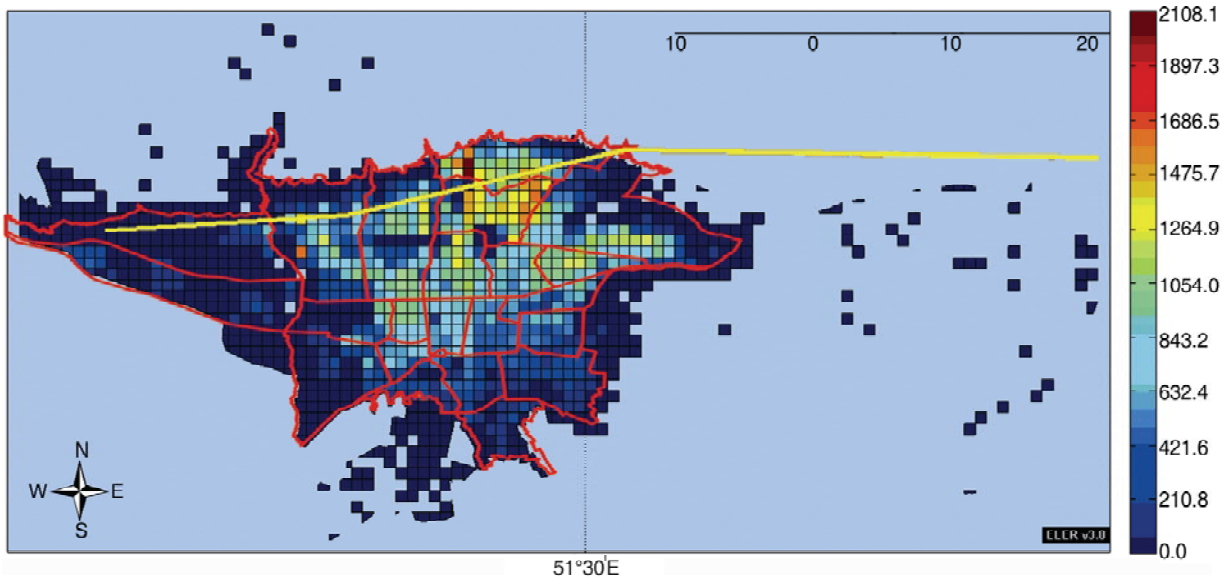

Figure 12. Distribution of damaged housing units for NTF scenario (Grades of D4+D5).

6. Case Study 2 - Ahar-Varzeghan Earthquake

Two earthquakes occurred in about eleven minutes on August 11, 2012 with moment magnitudes of 6.4 and 6.3 respectively. These events were detected at 23 km and 30 km west to Ahar and about 60 km North-East of Tabriz in East Azerbaijan province. According to the findings of the Institute of Geophysics at Tehran University (IGTU), and considering the fact that this institute manages a network of permanent seismic stations in the NW Iran (Tabriz

Table 5. Count of damaged residential housing units and casualties for scenario earthquakes.

Scenario Earthquake	Housing Unit Counts		Casualty Counts by Coburn and Spence (1992) Model	
	D5 Damage Grade	D4 and D5 Damage Grades	S4 Severity Level	S3 and S4 Severity Levels
North Tehran Fault - NTF	72580	349428	69349	100680
Rey Fault - RF	58277	257329	58683	54468
Mosha Fault - MF	4314	61223	6210	7901

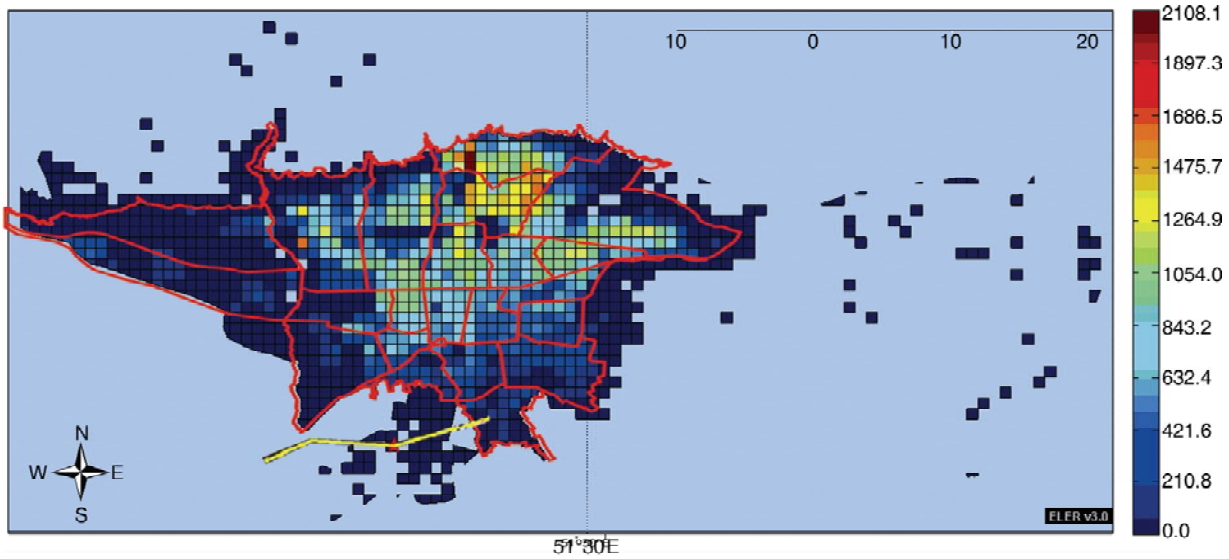

Figure 13. Distribution of damaged housing units for RF scenario (Grades of D4+D5).

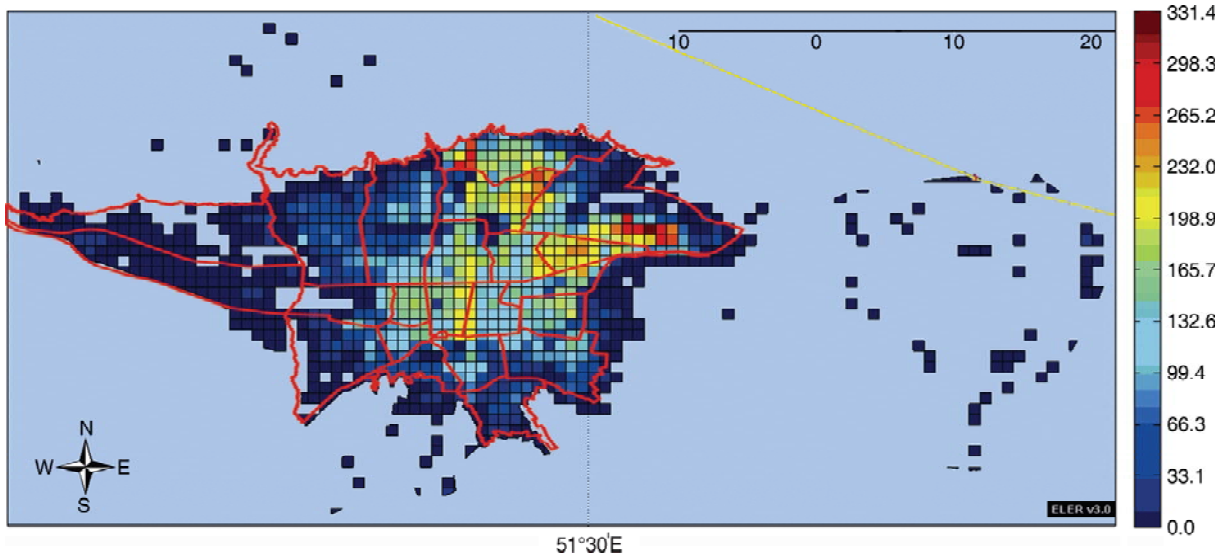

Figure 14. Distribution of damaged housing units for MF scenario (Grades of D4+D5).

Seismic Network), the focal depths of the first and the second shocks were determined with better accuracy as 9 and 16 km respectively [39]. For this, it is believed that the impact of the first earthquake has resulted in far more losses; therefore, this earthquake was chosen for the loss modeling. Nevertheless, the loss modeling as the impact of two consecutive earthquakes is nearly impossible at this time. Table (6) indicates the general description for these two events.

6.1. Fault and Intensity Distribution

Figure (15) shows the distribution of aftershocks within 100 km focal distance, Ahar fault and the surface rupture in the West-East direction. The focal mechanisms of both events are consistent with right-lateral strike-slip faulting on E-W trending in the shallow crust of the Eurasian plate [40].

In generating the shake map, the moment magnitude, the depth, the faulting mechanism and the rupture length are complemented together with the site effects. The method for taking into account the site effect (i.e. Vs30) and the ground motion prediction equations is similar to the case study of Tehran as described in the previous section. Figure (16) depicts the distribution of the instrumental intensity for Ahar-Varzeghan earthquake specific to the first event.

7. Distribution of Building Damage and Casualty for Ahar-Varzeghan Region

Considering the building and the population databases (as reported in previous sections) and the suggested vulnerability curves, Figure (7), Table (7) shows the estimated numbers for D5 and combined D4 and D5 damages (EMS-98 damage grades) to

Table 6. Ahar-Varzeghan Earthquakes' descriptions .

	Reference	UTC time	Lat.	Long.	Mag. type	Mag.	Depth
First Event	IIEES	12:23:16.2	38.550	46.870	Mw	6.4	10
	USGS	12:23:17.0	38.322	46.888	Mw	6.4	9.9
Second Event	IIEES	12:34:35.0	38.580	46.780	Mw	6.3	10
	USGS	12:34:35.0	38.324	46.759	Mw	6.3	9.8

IIEES: International Institute of Earthquake Engineering and Seismology
USGS: U.S. Geological Survey

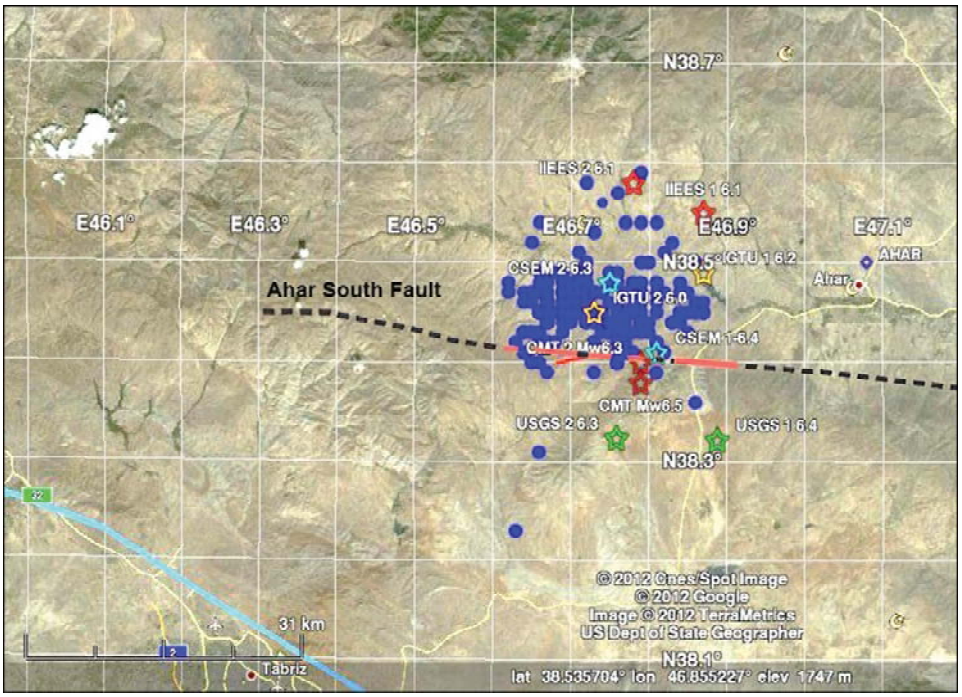

Figure 15. Surface rupture (reported by IIEES - http://www.iiees.ac.ir/English/) with aftershock distribution and suggested fault (http://supersites.earthobservations.org/ahar.php) overlaid on Google Earth map (courtesy of Google Earth).

the housing units for Ahar, Varzeghan and Heris regions.

Table (8) provides the actual number of building damage and casualty as reported by the "Building Foundation of East Azerbaijan" for three major high hit regions namely, Ahar, Varzeghan and Heris. According to a global model [39] the number of estimated deaths (S4) and the combined number for deaths (S4) and severely injured people (S3) are 320 and 725 respectively.

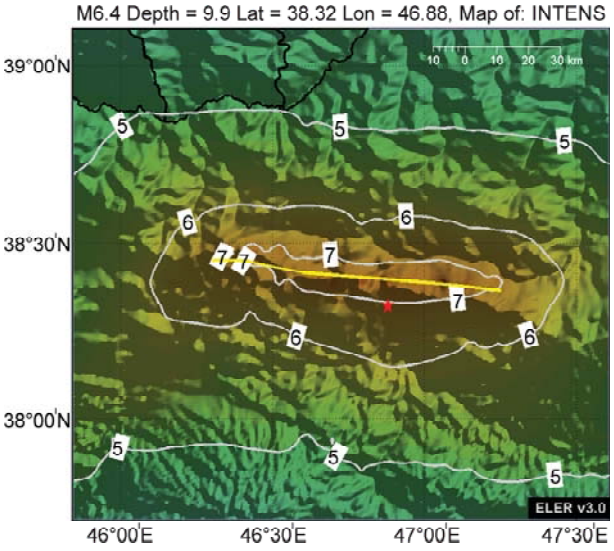

Figure 16. Intensity distribution Maps for Ahar-Varzeghan scenario (first event).

8. Conclusion

Taking into consideration that earthquake risk and disaster management strategic planning must be backed by scientific findings, the present research is aimed at providing a platform for estimating earthquake loss for the entire country focusing on the residential housing and human losses. A fast and easy-to-implement seismic risk assessment procedure is proposed in this study.

The geospatial information for building inventory and population were compiled and processed in order to generate a country-wide database in grid format. The shake maps are evaluated considering important faults, their specific parameters, the estimates of site conditions along with the use of suitable ground motion prediction equations. The vulnerability functions were derived studying the empirical data and analytical results for the building stock. As a result, the estimates of the number of damaged housing units and the related casualties are calculated for each grid.

Three major faults are considered accountable for major seismic loss for Tehran as case study one. The current findings show that if a destructive earthquake is caused by the North Tehran Fault, the estimated building and human losses (count of 349428 heavily damaged or destroyed housing units

Table 7. Building loss estimates according to D5 and D4+D5 damage grades.

Type of Building	S1		S2		S3		RC1		RC2		RC3		M1		M2-3		ADOBE	ALL
Damage State	D5	D4 + D5	D5	D4 + D5	D5	D4 + D5	D5	D4 + D5	D5	D4 + D5	D5	D4 + D5	D5	D4 + D5	D5	D4 + D5	D5	D4 + D5	SUM D5	SUM D4+D5
Ahar	4	101	44	562	8	80	0	7	0	3	0	0	9	201	487	2190	274	938	826	4082
Varzeghan	0	1	0	1	0	0	0	1	0	0	0	0	16	91	91	340	396	1624	503	2058
Heris	0	0	0	0	5	20	0	0	0	0	0	0	5	51	50	201	348	1348	403	1620
																		SUM	1732	7760

Table 8. Reported actual loss according to Building Foundation of East Azerbaijan.

Location (Township)	Village	Damaged Village	Casualty Category			Count of Buildings		
			Deaths	Seriously Injured	Lightly Injured	Damage Grade Ranges (%)		
						0-30	30-60	60-100
Ahar	305	97	38	250	500	1016	1571	2873
Varzeghan	157	106	120	600	1000	1617	2222	3924
Heris	101	78	96	250	1050	921	1110	4473
Sum	563	281	254	1100	2550	3554	4903	11270

and 69349 estimated deaths) outnumber the results for Mosha and Rey scenarios. For RF, 257329 heavily damaged or destroyed housing units and 58683 deaths are estimated. These figures are respectively 61223 and 6210 for MF. For case study two, the actual Ahar-Varzeghan earthquake of August 2012 is considered. The estimated numbers are 7760 for heavily damaged or destroyed housing units and 1045 for people suffering severe injuries or dead. According to an official report, these figures are 11270 for buildings and 1354 for human loss (severely injured or dead). It is notable that the developed database used in this study is specific to housing units rather than buildings. However, in rural areas (the case for Ahar, Varzeghan and Heris) the housing units and buildings can be regarded essentially comparable.

It is notable that in estimating earthquake risk to urban areas, there are numerous sources for uncertainties and errors primarily due to the nature of earthquake events and the lack of data, information, knowledge and restrictions in practical modeling. However, a successful country-wide platform must have the capability of updating the database with acceptable precision providing reasonable accurate results. The findings show that the model is prepared effectively for building taxonomy and population for Iran. The loss estimation results reveal that this proposed procedure provides an effective tool for risk and disaster managers to have a better understanding for predicting the outcomes of disastrous earthquakes.

Acknowledgements

This research is completed in part under the IIEES (International Institute of Earthquake Engineering and Seismology) internal contract #AM 7-269 (15/5/90) as part of the GEM-EMME contract with IIEES and their support is acknowledged. Some of the results were calculated using the ELER (Earthquake Loss Estimation Routine) software developed by KOERI (Kandili Observatory and Earthquake Research Institute - Bogazici University, Istanbul-Turkey). The LandScan program is owned by the Oak Ridge National Laboratory (ORNL), the data was made available through the GEM project and is acknowledged herein. The authors have benefited from Dr. Hessami-Azar (IIEES) comments and guidance with respect to evaluating the hazard sources.

References

1. RISK-UE (2003) An advanced approach to earthquake Risk Scenarios, with applications to different European cities, http://www.risk-ue.net.
2. Wald, D.J. and Allen, T.I. (2007) Topographic slope as a proxy for seismic site conditions and amplification. *Bulletin of the Seismological Society of America*, **97**(5), 1379-1395.
3. Wald, D.J., Worden, B.C., Quitoriano, V., and Pankow, K. (2005) Shake Map Manual: Techni cal Manual, User's Guide, and Software Guide. United States Geological Survey (USGS), CA, USA.
4. GDACS (Global Disaster Alert and Coordination System), http://www.gdacs.org).
5. WAPMERR (World Agency of Planetary Monitoring Earthquake Risk Reduction, http:// www.wapmerr.org.
6. PAGER (Prompt Assessment of Global Earthquakes for Response), http://earthquake.usgs.gov/ eqcenter/pager/, system of USGS.
7. Eguchi, R.T., Goltz, J.D., Seligson, H.A., Flores, P.J., Blais, N.C., Heaton, T.H., and Bortugno, E. (1997) Real-time loss estimation as an emergency response decision support system, the early post-earthquake damage assessment tool (EPEDAT). *Earthquake Spectra*, **13**(4), 815-833.
8. Larionov, V., Frolova, N., and Ugarov, A. (2000) 'Approaches to vulnerability evaluation and their application for operative forecast of earthquake consequences'. In: Ragozin A (ed) All-Russian conference "Risk-2000". Ankil, Moscow, 132-135.
9. HAZUS-MH (2003) Multi-hazard Loss Estimation Methodology, Earthquake Model, HAZUS® MH, Technical Manual National Institute of Building Sciences and Federal Emergency Management Agency (NIBS and FEMA), Washington, DC, 690p.
10. MATLAB (2008) R2008b, the Math Works, Inc.
11. Elnashai, A.S., Hampton, S., Karaman, H., Lee,

J.S., Mclaren, T., Myers, J., Navarro, C., Sahin, M., Spencer, B., and Tolbert, N. (2008) Overview and applications of Maeviz-Hazturk 2007. *Journal of Earthquake Engineering*, **12**(S2), 100-108.

12. Zonno, G., Garcia-Fernandez, M., Jimenez, M.J., Menoni, S., Meroni, F., and Petrini, V. (2003) The SERGISAI procedure for seismic risk assessment. *Journal of Seismology*, **7**, 259-277.

13. Sabetta, F., Goretti, A., and Lucantoni, A. (1998) Empirical fragility curves from damage surveys and estimated strong ground motion. *11th European Conference on Earthquake Engineering*, Paris.

14. Susagna, T., Goula, X., Roca, A., Pujades, L., Gasulla, N., and Palma, J.J. (2006) Loss scenarios for regional emergency plans: application to Catalonia, Spain. *Assessing and Managing Earthquake Risk*, C.S. Oliveira, A. Roca and X. Goula, Editors., 463-478.

15. Dominique, P., Goula, X., Colas, B., Jara, J.A., Romeu, N., Susagna, T., Irizarry, J., Sedan, O., Figueras, S., Roullé, A., and Olivera, C. (2007) Système transfrontalier de réponse rapide en cas de séisme dans les Pyrénées Orientales. *7ème Colloque National de l'AFPS*, Paris, CD-ROM, Paper ID V-143. [in French].

16. Barranco, L. and Izquierdo, A. (2002) SES 2002 - Software for the Rapid Preliminary Estimation of Potential Damage caused by earthquakes in Spain., Spanish Civil Protection and National Geographic Institute of Spain [in Spanish].

17. ELER (Earthquake Loss Estimation Routine) (2010) Technical Manual and Users Guide of ELER© v3.0, Prepared by Bogazici University, Department of Earthquake Engineering Istanbul.

18. GEM. (2010), "Global Earthquake Model". http://www.globalquakemodel.org.

19. Erdik, M., Aydinoglu, N., Fahjan, Y., Sesetyan, K., Demircioglu, M., Siyahi, B., Durukal, E., Ozbey, C., Biro, Y., Akman, H., and Yuzugullu, O. (2002) Earthquake risk assessment for Istanbul Metropolitan Area. Bogazici University, Kandilli Observatory and Earthquake Research Institute, Istanbul, Rep. No. 16, http://www.koeri.boun.edu.tr/depremmuh/EXEC ENG.pdf.

20. LandScan, High Resolution Global Population Data Set, Oak Ridge National Laboratory, Oak Ridge, TN <http://www.ornl.gov/sci/landscan/>.

21. Mansouri, B. and Amini-Hosseini, K. (2014) Development of Residential Building Stock and Population Databases and Modeling the Residential Occupancy Rate for Iran. Natural Hazards Reviews, doi: 10.1061(ASCE)NH. 1527-6996.0000109, **15**(1), ISSN 1527-6988.

22. Tavakoli, B. and Tavakoli, S. (1993) Estimating the vulnerability and loss functions of residential buildings. *Natural Hazards*, **7**(2), 155-171.

23. JICA (2000) Japan International Cooperation Agency. The Study on Seismic Microzoning of the Greater Tehran Area in the Islamic Republic of Iran, Final Report, Main Report, SSF JR 00-186.

24. Grunthal, G. (1998) European Macroseismic Scale. Cahiers du Centre Europ´een de G´eodynamiqueet de S´eismologie. Conseil de l'Europe. Luxembourg.

25. Mansouri, B., Ghafory-Ashtiany, M., Amini-Hosseini, K., Nourjou, R., and Mousavi, M. (2010) Building seismic loss model for Tehran, Earthquake Spectra. *Journal of Earthquake Engineering Research Institute (EERI)*, **26**(1), 153-168.

26. Kircher, C.A., Nassar, A.A., Kustu, O., and Holmes, W.T. (1997) Development of building damage functions for earthquake loss estimation. *Earthquake Spectra*, **13**, 663-681.

27. Mansouri, B. and Kiani A. (2011) Development of structural fragility curves considering the site condition for Tehran. *6th International Conf. on Seismology and Earthquake Engineering*, UR 11322, Tehran.

28. ATC-13 (1987) Applied Technology Council. Earthquake damage evaluation data for California, Redwood City, California.

29. Trifunac, M.D. and Brady, A.G. (1975) On the correlation of seismoscope response with earth-

quake magnitude and modified mercalli intensity. *Bulletin of Seismological Society of America*, **65**(2).

30. Porter, K.A., Jaiswal, K., Wald, D.J., Earle, P.S., and Hearne, M. (2008) Fatality models for the U.S. geological survey's prompt assessment of global earthquakes for response, (PAGER) System. *Proc. 14th World Conf. on Earthquake Engineering*, Beijing, China, paper S04-009.

31. JICA (2004) Japan International Cooperation Agency. Tehran Master Plan.

32. Donald, L., Wells, D.L., and Coppersmith, K.J. (1994) New empirical relationships among magnitude, rupture length, rupture width, rupture area, and surface displacement, *Bulletin of the Seismological Society of America*, **84**(4), 974-1002.

33. Gholipour, Y., Bozorgnia, Y., Rahnama, M., Berberian, M., Ghoreishi, M., Talebian N., Shaja-Taheri, J., and Shafeei, A. (2011) Probabilistic Seismic Hazard Analysis Phase I - Greater Tehran Regions. Final Report - University of Tehran.

34. Djamour, Y., Vernant, P., Bayer, R., Nankali, H.R., Ritz, J.F., Hinderer, J., Hatam, Y., Luck, B., L.e., Moigne, N., Sedighi, M. and Khorrami, F. (2010) GPS and gravity constraints on continental deformation in the Alborz mountain range, Iran. *Geophysical Journal International*, **183**, 1287-1301.

35. Shafiee, A. and Azadi, A. (2007) Shear-wave velocity characteristics of geological units throughout Tehran City, Iran. *Journal of Asian Earth Sciences*, **29**(1), 105-115.

36. Ghayamghamian, M.R., Mansouri, B., Amini-Hosseini, K., Tasnimi, A.A., Haghshenas, E., and Govahi, N. (2011) Determination of Seismic Site Amplification Factors and the Derivation of Structural Fragility Curves and Casualty Functions for Tehran Building Stock, Tehran Disaster Mitigation and Management Organization, TDMMO - Municipality of Tehran.

37. Boore, D.M., Joyner W.B., and Fumal, T.E. (1997) Equations for estimating horizontal response spectra and peak accelerations from western north american earthquakes. A Summary of Recent Work, Seism Res Lett, **68**, 128-153.

38. Walled et al. (1999).. ????????????

39. Coburn, A. and Spence, R. (1992) *Earthquake Protection*. John Wiley & Sons.

40. Razzaghi, S.M. and Ghafory-Ashtiany, M. (2012) A Preliminary Reconnaissance Report on August 11th 2012, Varzaghan-Ahar Twin Earthquakes in NW of Iran.